BULLETIN
OF THE
CHEMICAL SOCIETY OF JAPAN

**On the Origin and Structure of the Recently Observed Acetal in the Soai Reaction**

Ilya D. Gridnev* and Andrey Kh. Vorobiev*

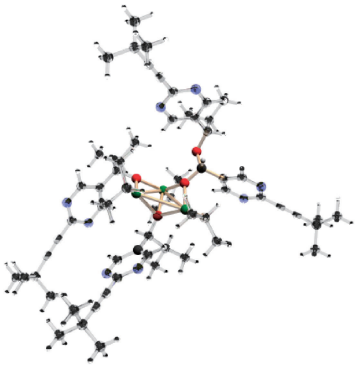

The acetal species recently observed in the course of the Soai reaction was identified as a kinetically stable off-loop species. DFT search for the appropriate structures revealed a $Zn_3$-cluster as the most possible candidate.

*Bull. Chem. Soc. Jpn.*
1–8

BCSJ

# On the Origin and Structure of the Recently Observed Acetal in the Soai Reaction

**Ilya D. Gridnev*[1] and Andrey Kh. Vorobiev*[2]**

[1]Department of Chemistry, Graduate School of Science, Tohoku University, Sendai, Miyagi 980-8578

[2]Department of Chemistry, Moscow State University, Vorobievy Gory, Moscow 119991, Russia

E-mail: igridnev@m.tohoku.ac.jp
Received: November 4, 2014; Accepted: November 17, 2014; Web Released: xxxxx xx, xxxx

Recent observation of the acetal species in the course of autoamplifying Soai reaction was analysed by the formal kinetic analysis of the experimental data and DFT computations. Kinetic analysis demonstrated convincingly that the observed species cannot be a precursor of the reaction product. Hence, it is an off-loop species that is not important for the process of the chirality amplification. DFT search for a kinetically stable acetal species resulted in the location of a $Zn_3$ cluster stabilized with three Zn–O–Zn bridges.

The widespread interest in the mechanism of the Soai reaction (Scheme 1),[1–5] the only known straightforward example of self-amplifying autocatalytic reaction, is mostly stipulated by its possible connection to the emergence of homochirality in the biosphere.[6–10] Although it is well recognized that physicochemically the phenomenon of a self-amplifying autocatalysis must be based on some of the numerous possible modified Frank schemes,[11–23] the intrinsic nature of the chemical processes that make possible effective amplification of the enantiomeric excess is much less clear.

Recently Brown, Blackmond, et al. reported observation of a transient intermediate in the Soai reaction.[24] Although the exact structure of the observed species remained elusive, it was possible to demonstrate that it definitely contains an acetal fragment. However, no suggestions of the origin of this transient species have been made. Nor has the relevance of this species to any amplifying catalytic cycle of the Soai reaction been discussed.

Hence, three questions are posed by the publication of the paper cited as Ref. 24:

1. Is the acetal species an important intermediate in the amplifying catalytic cycle of the Soai reaction? Must then any catalytic cycle suggested for this reaction contain an acetal intermediate?

2. If this is not the case, how can the kinetics of accumulation and decay of the acetal be explained?

3. What are the origin and the structure of the acetal species?

In this work we argue that the experimental kinetic curves reported in[24] (Figures 1a and 1b) contain enough information to identify the acetal as an out-of-loop species in the catalytic cycle, as well as to discriminate between two possible kinetic schemes for the formation of an off-loop species. We also suggest a possible structure of the acetal being a kinetically trapped $Zn_3$ cluster, and simulate the kinetics of its formation from a pentameric product.[25]

Our approach to the problem involves formal kinetic analysis of the available data, DFT (density functional theory) computation of the possible intermediates and transition states followed by the kinetic simulation of the kinetic curves using the thermodynamic parameters obtained computationally and comparison of the calculated kinetic curves to the experimental ones.

The recent developments of the DFT methods resulted in the possibility to compute accurately various thermodynamic and kinetic parameters of organic and organometallic reactions in a reasonable agreement with experiments, provided that an appropriate computational method is used.[26–34] In our previous publication on the mechanism of the Soai reaction we have shown by careful comparison with the experimental data and other computational methods that the use of B3LYP/6-31G*(cpcm, toluene) level of theory adequately describes sophisticated equilibria in the reaction pool of the Soai reaction.[25] Hence, we reasoned that the same computational method can be used for unravelling the nature of the acetal species and its role in the autoamplifying reaction.

The kinetics of the acetal concentration decay at large times[24] can be used for the rough estimation of the correspond-

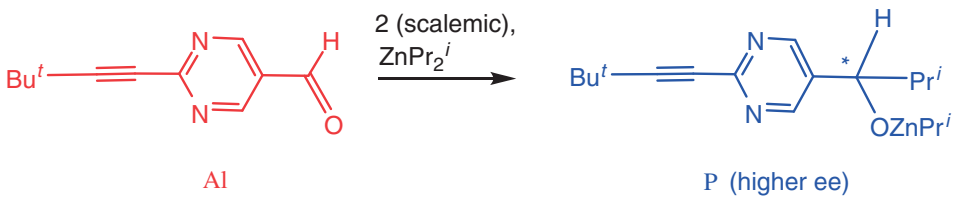


Al P (higher ee)

**Scheme 1.** The Soai reaction.


 

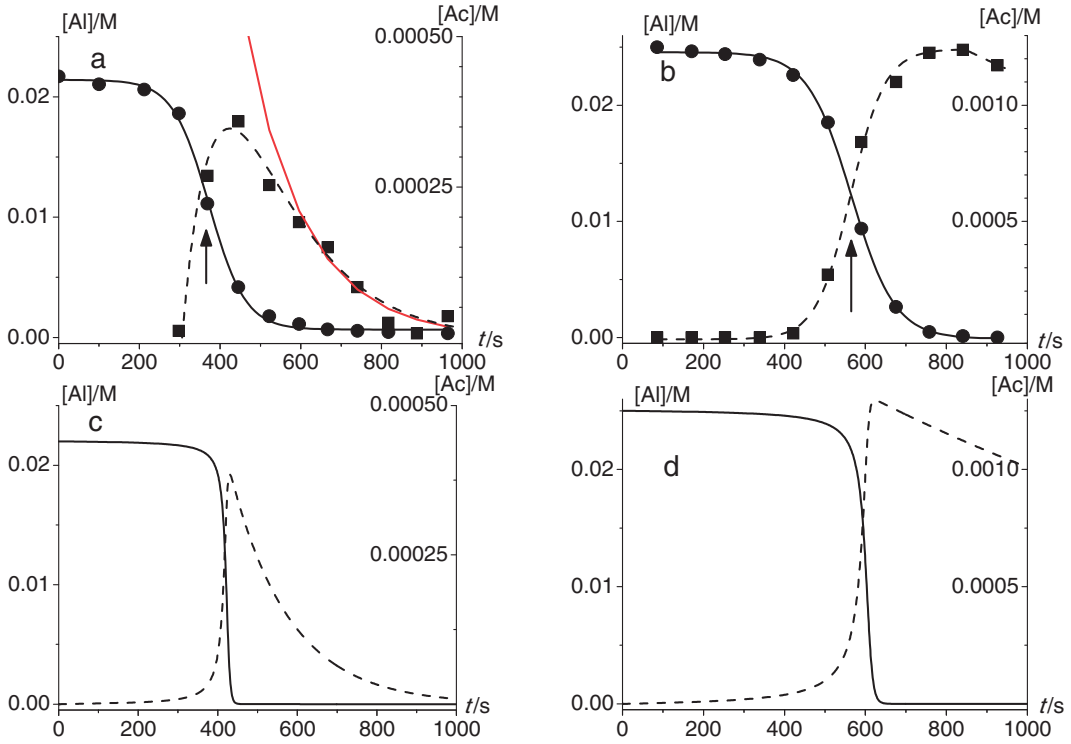


**Figure 1.** Kinetic curves for the aldehyde decay (dots) and acetal formation at 273 (a) and 253 K (b). Experimental data points were taken from Ref. 24. The arrows show the conciding points of the maximal rates of the acetal formation and aldehyde decay. Results of modeling the kinetic curves are (c) and (d) respectively. Conditions: [Al] 0.022 M, $Pr_2^iZn$ 0.044 M, starting concentration $[P]_0$ 0.0011 M, toluene-$d_8$. The red curve in the Figure 1a shows kinetics of a monomolecular decay with $k_{d,Ac} = 6.7 \times 10^{-3}\,s^{-1}$.

**Table 1.** Estimations of the Rate Constants and Activation Energy for the Acetal Decay

| $T$/K | $k_{d,Ac}/s^{-1}$ |
|---|---|
| 273[a)] | $(6.7 \pm 1.9) \times 10^{-3}$ |
| 253[b)] | $(6.8 \pm 1.9) \times 10^{-4}$ |
| $E_a = 15.9 \pm 4.0$ kcal mol$^{-1}$ | |

a) Obtained assuming monomolecular decay of the acetal at large times (red curve in the Figure 1a). Evaluation of the possibility of a bimolecular decay is given in ESI. b) Obtained from last two points of the experimental kinetic curve in the Figure 1b.

ing rate constants and effective activation energy (Table 1). It should be noted that the following kinetic analysis is not sensible to the accurateness of the values listed in Table 1, whereas the estimation of the rate constants on the necessary level of the magnitude order is quite reliable.

We have considered three possible kinetic schemes of the acetal formation:

1. Acetal is a precursor of the reaction product in the catalytic cycle, i.e. it is being produced via a consecutive route (Scheme 2): In this case the kinetics of the acetal formation is described by the following equations:

$$\frac{d[Al]}{dt} = -f(k, [Al], [cat], [reactant])$$
$$\frac{d[Ac]}{dt} = f(k, [Al], [cat], [reactant]) - k_{d,Ac}[Ac] \quad (1)$$


**Scheme 2.** Al is the starting aldehyde, Ac is the acetal, and P reaction product.

where $k_{d,Ac}$ is the rate constant of the acetal decay, and the function $f(k,[Al],[cat],[reactant])$ describes the formation of the acetal from the starting aldehyde in the first stage of the consecutive kinetic scheme.

Substituting the first equation in the second equation in eq 1 one can obtain the following:

$$\frac{d[Ac]}{dt} = -\frac{d[Al]}{dt} - k_{d,Ac}[Ac] \quad (2)$$

Formal integration of eq 2 yields the following expression:

$$\int_0^t \frac{d[Ac]}{dt}\,dt = -\int_0^t \frac{d[Al]}{dt}\,dt - \int_0^t k_{d,Ac}[Ac]dt \quad (3)$$

Taking into account the absence of the acetal in the initial solution $[Ac]_0 = 0$, the left side of eq 3 can be expressed as:

$$\int_0^t \frac{d[Ac]}{dt}\,dt = [Ac]_t - [Ac]_0 = [Ac]_t \quad (4)$$

First term in the right side of eq 3 is:

$$-\int_0^t \frac{d[Al]}{dt}\,dt = -[Al]_t + [Al]_0 \quad (5)$$

Second term in in the right side of eq 3 is:

**Table 2.** Specific Features of the Acetal Formation Computed Assuming its Participation in the Catalytic Cycle Compared to the Experimental Values

| $T$/K | $t$/s | $([Al]_0 - [Al]_t)$ | $k_{d,Ac}$ | $\sum_i [Ac]_i \Delta t_i$ | $k_{d,Ac} \sum_i [Ac]_i \Delta t_i$ | $[Ac]_{calcd}$ | $[Ac]_{exper.}$ |
|---|---|---|---|---|---|---|---|
| 253 | 926 | 0.025 | $6.8 \times 10^{-4}$ | 0.4429 | $3 \times 10^{-4}$ | 0.0247 | $1.2 \times 10^{-3}$ |
| 273 | 445 | 0.0175 | $6.7 \times 10^{-3}$ | 0.0345 | $2.3 \times 10^{-4}$ | 0.0173 | $3.6 \times 10^{-4}$ |
| 273 | 964 | 0.0217 | $6.7 \times 10^{-3}$ | 0.1019 | $6.8 \times 10^{-4}$ | 0.0210 | $3.5 \times 10^{-5}$ |

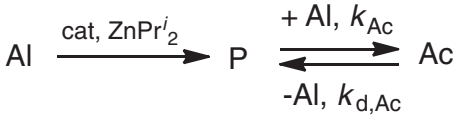


**Scheme 3.**

$$-\int_0^t k_{d,Ac}[Ac]dt = -k_{d,Ac}\int_0^t [Ac]dt \quad (6)$$

By combing eqs 4, 5, and 6:

$$[Ac]_t = ([Al]_0 - [Al]_t) - k_{d,Ac}\int_0^t [Ac]dt \quad (7)$$

For practical use the integral in the eq 7 can be changed to a sum:

$$\int_0^t [Ac]dt = \sum_i [Ac]_i \Delta t_i$$

$$[Ac]_t = ([Al]_0 - [Al]_t) - k_{d,Ac}\sum_i [Ac]_i \Delta t_i \quad (8)$$

and eq 7 is transformed to eq 8, which can be directly used for the comparison of the calculated and experimental values of the acetal concentrations (Table 2).

Data presented in Table 2 show that experimental acetal concentrations are incompatible with eq 8. Substitution of the experimental running concentrations in the right part of eq 8 lead to the calculated values $[Ac]_{calc}$ which are overestimated by several orders of magnitude. Indeed, because of the relatively low value of the decay rate constant, the consecutive scheme implies that all reacted aldehyde must remain in the acetal form for a considerable time span. Experiment does not confirm this feature. Hence, we can reliably conclude that the acetal is not formed via the consecutive scheme and is not a precursor of the product within the catalytic cycle. This conclusion remains valid for a quite wide range of the acetal decay rate constants and for bimolecular acetal decay as well.

It should be noted that no additional assumptions have been made for the kinetic scheme shown in Scheme 2, hence the above conclusion makes possible a definite answer for the first question: *the acetal species is not an important intermediate in the amplifying cycle of the Soai reaction*. The other two possible kinetic schemes explaining the experimental detection of the acetal consider it as an off-loop species of the catalytic cycle.

2. Formation of the acetal from the reaction product and remaining aldehyde (Scheme 3): In terms of this model the kinetic equation for a bimolecular acetal formation can be drawn in the following way:

$$\frac{d[Ac]}{dt} = k_{Ac}[P][Al] - k_{d,Ac}[Ac] \quad (9)$$

where $k_{Ac}$ is the rate constant of the acetal formation.

The decrease of the concentration of acetal at large times occurs in this case due to the decrease of the aldehyde concentration. When the concentration of acetal reaches its maximum, the right part of the eq 9 should be equal to zero giving the rate constant for the acetal formation:

$$k_{Ac} = \left(\frac{k_{d,Ac}[Ac]}{[P][Al]}\right)_{t_{max}} \quad (10)$$

where all concentrations are taken at the time of the maximal acetal concentration.

Equation 10 allows estimation of the rate constant $k_{Ac}$. Applying the corresponding values yields $k_{Ac}(273) = 0.033$ $M^{-1}\,s^{-1}$ and $k_{Ac}(253) = 0.28\,M^{-1}\,s^{-1}$ exhibiting an unusual temperature dependence. Moreover, the maximal acetal concentrations in terms of this kinetic scheme must be observed at the maximal values of the product [P] [Al], i.e. at 50% conversion. The experimental kinetic data are in disagreement with this prediction, especially at 253 K (Figure 1b).

Although the discrepancies between the experimental observations and simulated kinetics of this kinetic scheme are not as significant as in the case of the consecutive formation of the product, the evident deviations of the maximal acetal concentrations from the 50% conversion points make this scenario doubtful. To further check the possibility of realization of this kinetic scheme we have undertaken the DFT calculations of the acetals which could be formed by product molecules. The most evident possibility is the acetal forming by the reaction of the square dimer $P_2$ with aldehyde via the corresponding adduct $P_2 \cdot Al$ (Scheme 4).[24] Formally, these transformations correspond to the kinetic scenario shown in Scheme 3.

We have computed the equilibria showed in the Scheme 4; the results are collected in the Table 3.

The values of the reaction Gibbs energy in the Table 3 demonstrate that acetal formation from dimer product is thermodynamically forbidden. The estimations of rate constants prove slow formation and rapid destruction of the acetal formed by the dimer product. Similarly, the product of the reaction of aldehyde with the monomer P was found to be prone to rapid reverse reaction regenerating the starting compound and cannot be the source of acetal in noticeable amounts. Evidently, this conclusion is also valid for any other oligomer containing an acetal fragment lacking any additional structural stabilization. Thus the combination of kinetic and structural data strongly evidenced against this scenario.

3. Acetal is obtained from the same intermediate as the reaction product and yields itself the reaction product after decay (Scheme 5): In this case the maximal rate of the acetal formation must be observed at the moment of the maximal rate of the aldehyde decay that nicely corresponds to the experimental kinetic observations, since the points of the maximal


 

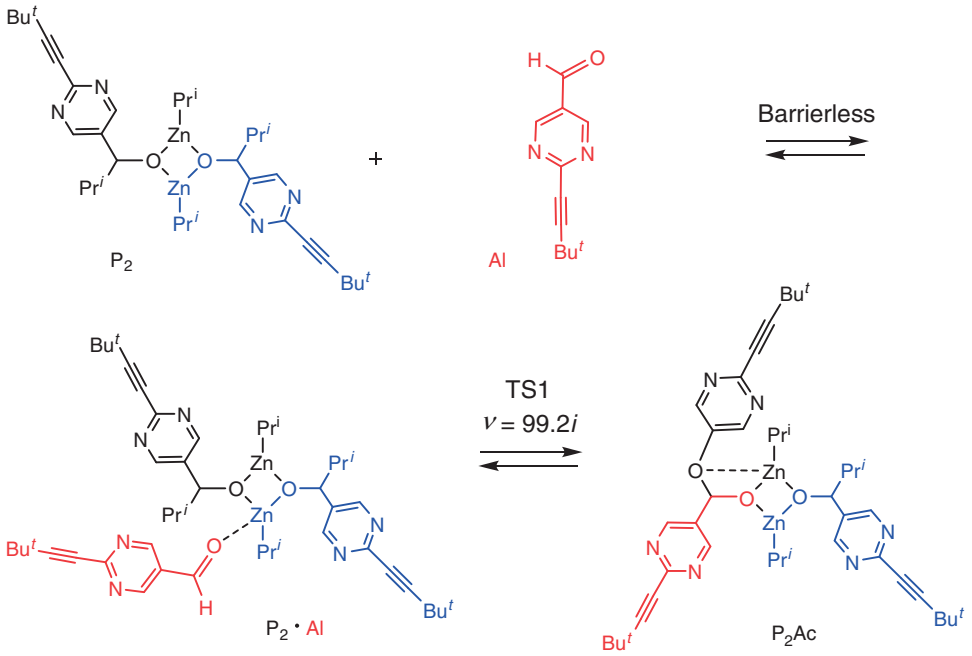


**Scheme 4.**

**Table 3.** Computed Gibbs Energies and Gibbs Activation Energies for the Formation of Acetal

| $T$/K | $\Delta G$/kcal mol$^{-1}$ $P_2 + Al \rightarrow P_2Ac$ | $\Delta G^{\neq}$/kcal mol$^{-1}$ $P_2 + Al \rightarrow P_2Ac$ | $k_{Ac}$ [a]/M$^{-1}$ s$^{-1}$ | $\Delta G^{\neq}$/kcal mol$^{-1}$ $P_2Ac \rightarrow P_2 + Al$ | $k_{d,Ac}$ [a]/s$^{-1}$ |
|---|---|---|---|---|---|
| 273 | 8.6 | 11.5 | 0.7 | 10.7 | $3 \times 10^3$ |
| 253 | 7.6 | 8.6 | 41.5 | 10.7 | $6 \times 10^2$ |

a) The pre-exponential factors for monomolecular and bimolecular rate constants presented in Table 3 were assumed to be $10^{12}$ s$^{-1}$ and $10^9$ M$^{-1}$ s$^{-1}$, respectively.

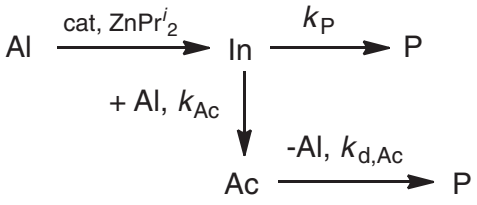


**Scheme 5.**

rates of the acetal formation and aldehyde decay coincide (arrows in the Figure 1a and Figure 1b). The concentration of acetal is determined by the relative values of the rate constants $k_P$ and $k_{Ac}$.

Thus, this kinetic scheme does not contradict the experimental observations. It also gives certain hints for the possible structures of the intermediate and the acetal. The latter must form from an intermediate of the main catalytic cycle, give the same product after decomposition, and be thermodynamically unstable relative to decay, but kinetically long-living molecule to demonstrate the observed slow decay reaction with activation energy ca. 16 kcal mol$^{-1}$. Besides, according to the experimental data, it must be able to regenerate the aldehyde reversibly.[24] This is a rather strict set of criteria to meet, so we hoped to be able to identify a matching structure among the numerous possibilities.

Recently we have reported detailed study of the reaction pool of the Soai reaction that resulted in the formulation of a catalytic cycle consistent with all known structural, kinetic and amplifying properties of Soai reaction.[25] The immediate product of the stereospecific alkyl transfer within this catalytic cycle is an adduct of the tetrameric catalyst $P_4$ and monomeric alcoholate P. Under conditions of thermodynamic equilibrium the most stable species existing in the reaction pool of the Soai reaction are square Zn–O–Zn–O dimers, whereas monomeric or any "uneven" alcoholates (monomers, trimers, pentamers, ets.) are disfavored.[25,35–38] Therefore, to reach the thermodynamic equilibrium, the adduct $P_4$·P formed in the catalytic cycle must react with another molecule of P either directly or via dissociation to P and $P_4$ to yield the square dimer $P_2$ (Scheme 6). We reasoned further that in the presence of significant concentrations of the starting aldehyde, it could also react with the pentamer $P_4$·P yielding adduct $P_5$·Ac (Scheme 6).

Indeed, we have found by DFT computations that the formation of the acetal fragment can proceed through TS2 from $P_4$·P and Al with low activation barrier ($\Delta G^{\neq}(298) = 6.4$ kcal mol$^{-1}$) affording adduct of the catalyst and acetal $P_5$·Ac (Scheme 6). However, the reaction is reversible and the kinetic simulations showed that it is impossible to accumulate detectable concentrations of the acetal via this route, since the system very rapidly achieves the resting state consisting of square dimers $P_2$ and aldehyde.

We have undertaken the systematic search of stable acetal species with different (from one up to five) number of mono-

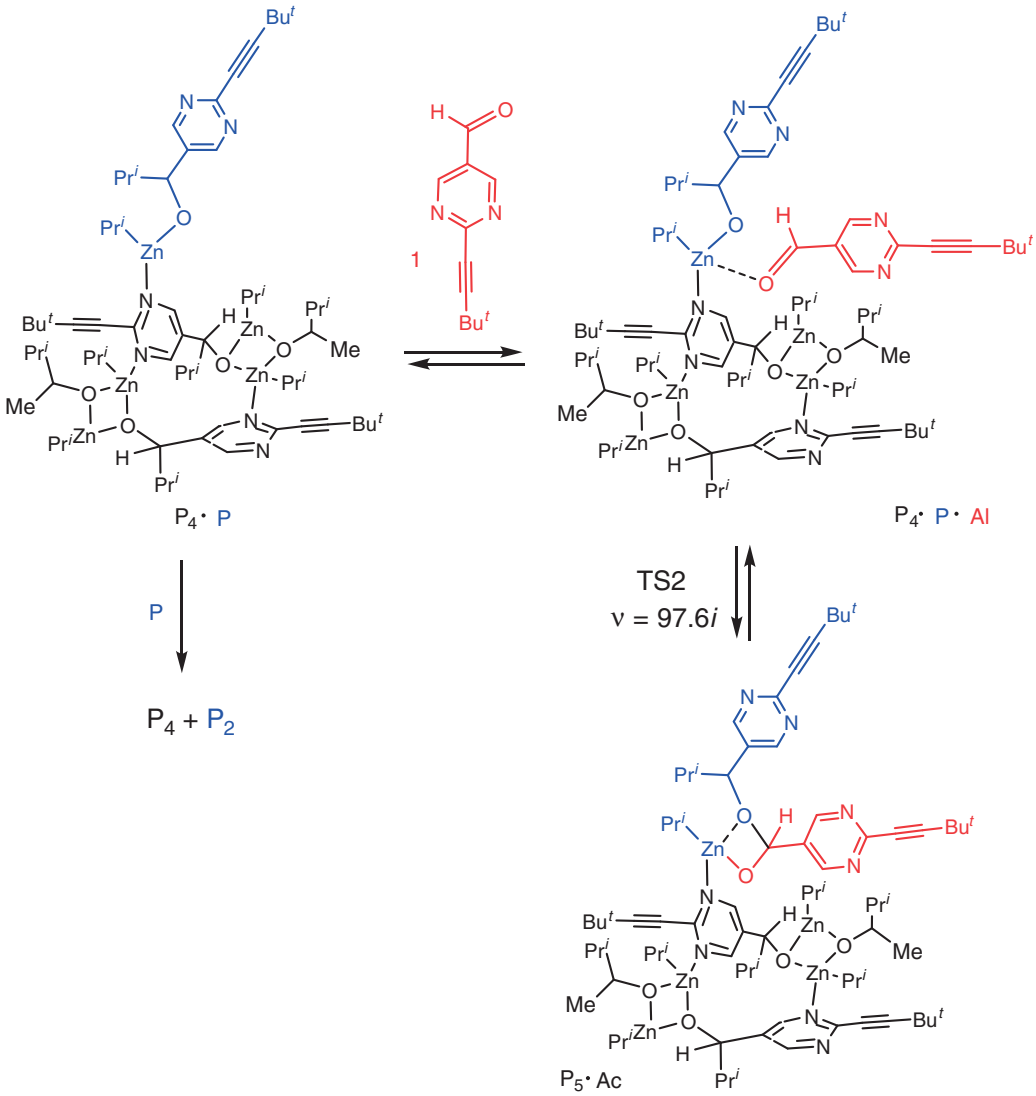


**Scheme 6.**

mer product units. Only the acetal $P_3$·Ac was found to be kinetically stable due to the formation of a $Zn_3$ cluster with close values of three Zn–Zn bond lengths (Figure 2).

Hence, we concluded that immediately after formation of the adduct $P_5$·Ac it can produce a more stable combination $P_2 + P_3Ac$ (Scheme 7).

The activation barrier for the recovery of Al from $P_3Ac$ was computed to be $\Delta G^{\neq}(298) = 25.3\,\text{kcal mol}^{-1}$, i.e. it was high enough to explain the kinetic trapping of acetal in $P_3Ac$, but too high to explain the kinetics of the acetal decay.

On the other hand, we have found that $P_3Ac$ is capable of dissociating to PAc and $P_2$ with effective activation barrier below $20\,\text{kcal mol}^{-1}$ (Scheme 7 and Figure 3). The dissociation followed by the rapid aldehyde recovery in PAc stands in a reasonable quantitative agreement with the velocity of the decay of the acetal species.

Thus the computational results are consistent with the modified kinetic scheme (Scheme 8).

In previous work we have shown that the kinetic features of the Soai reaction can be reasonably described in a quasi-stationary approximation. It implies that the equilibrium

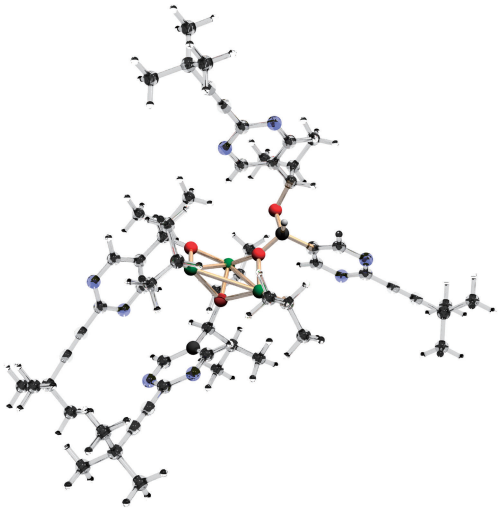

**Figure 2.** Optimized structure of the acetal $P_3$·Ac: zinc, green; oxygen, – red, nitrogen; blue, carbon; black, hydrogen – white. The Zn–Zn interatomic distances are 3.02, 3.09 and 3.19 Å.


 

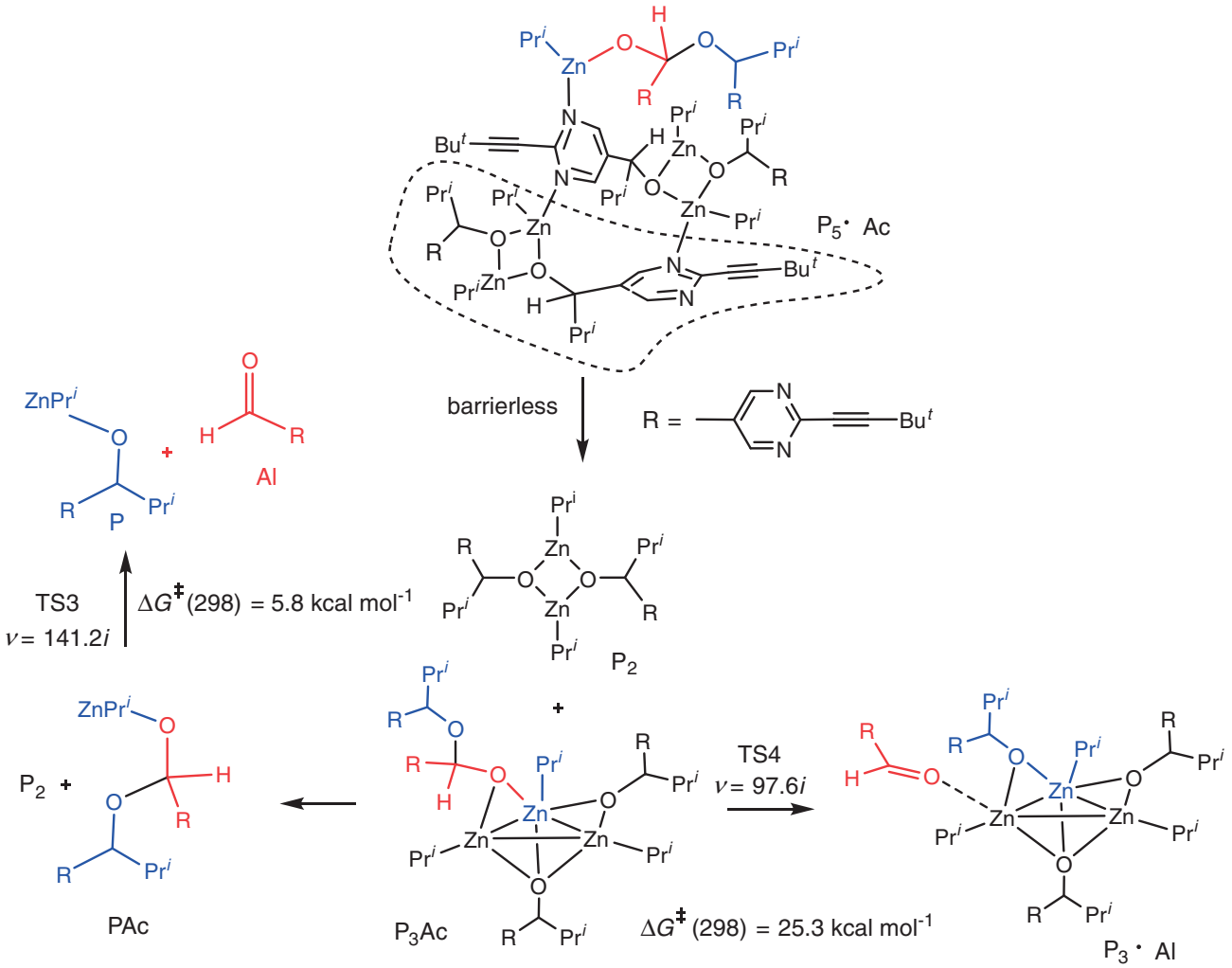


**Scheme 7.**

between various oligomers of alcoholate is much faster than the rate limiting catalytic stage of the reaction. Within this approximation the kinetics of the aldehyde decay is described by the eqs 11:[25]

$$\frac{d[C]}{dt} = ([C]_0 + [Al]_0 - [C])\cdot[Zn]\cdot[4k_r[P_2]^2((1+ee)^4 - (1-ee)^4) + 2k_0]$$
$$\frac{dee}{dt} = \frac{([C]_0 + [Al]_0 - [C])\cdot[Zn]\cdot[P_2]}{1 + K_{DZn}[Zn]}\left[2k_r\cdot((1+ee)^4(1-ee) - (1-ee)^4(1+ee)) - \frac{k_0\cdot ee}{K_D^2}\right] \quad (11)$$

where $[C]_0$, [C] are starting and running concentrations of the reaction product (total for all oligomers) expressed in moles of monomer, $[Al]_0$ is starting concentration of aldehyde, $k_0$ and $k_r$ is effective rate constants of background and catalytic alkylations, [Zn] is concentration of diisopropyl zinc, $K_{DZn}$ is equilibrium constant for binding of diisopropyl zinc with the square dimer $P_2$, $[P_2]$ is concentration of dimers that is calculated from the material balance conditions, $K_D$ is equilibrium constant for product dimerization, *ee* is enantiomeric excess.

In our case $ee = 1$. The further simplification of the eqs 11 is possible if we assume that $P_2$ is the major component of the oligomeric mixture and neglect the concentrations of other oligomers and their complexes with diisopropyl zinc. We also assume that the background reaction is much slower than the catalytic reaction. In these approximations the eqs 11 give for the Scheme 5:

$$\frac{d[Al]}{dt} = -k_r[Al]\cdot[Zn]\cdot[P_2]^2 - k_{Ac}[Al]\cdot[In] + k_{d,Ac}[Ac]$$
$$\frac{d[In]}{dt} = k_r[Al]\cdot[Zn]\cdot[P_2]^2 - k_{Ac}[Al]\cdot[In] - k_P[In]$$
$$\frac{d[Ac]}{dt} = k_{Ac}[Al]\cdot[In] - k_{d,Ac}[Ac] \quad (12)$$

where [In] is the concentration of the intermediate, [Ac] – concentration of acetal in the form $P_3$·Ac, and the concentrations [Zn] and $[P_2]$ are determined from the conditions of the material balance:

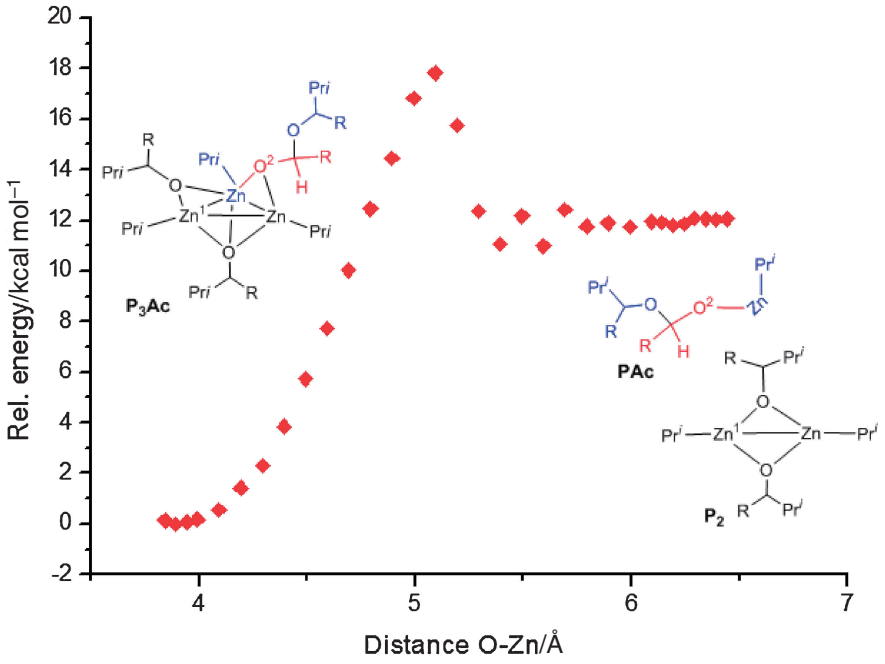


**Figure 3.** Scan of the relative energy versus the interatomic distance $Zn^1$-$O^2$ dissociation of the acetal $P_3$·Ac yielding $P_2$ and PAc requires overcoming the activation barrier of 17.8 kcal/mol. Complete dissociation occurs when the distance $Zn^1$-$O^2$ reaches 6 Å. Oscillations of the energy values observed at 5.5–6 Å are explained by weak intermolecular interactions between other Zn and O (N) atoms existing at certain values of the $Zn^1$–$O^2$ distance.

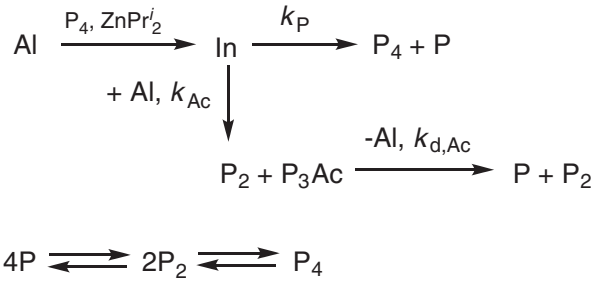


**Scheme 8.**

$$[Zn] = [Zn]_0 - [Al]_0 + [Al] + [Ac]$$
$$[P_2] = ([C]_0 + [Al]_0 - [Al] - 5[In] - 4[Ac])/2 \qquad (13)$$

The kinetics of the aldehyde decay and of the acetal formation was simulated via numerical solution of the eqs 12 and 13 as it is shown in Figure 1c and Figure 1d. The rate constants of the acetal decay shown in the Table 1 were used in the simulations. The values $k_r$ were adjusted to scale the reaction times to the experimental ones; their values were $1 \times 10^5$ and $7.2 \times 10^4$ for 273 and 253 K respectively. The absolute values of the rate constants $k_{Ac}$ and $k_P$ do not affect the shapes of the kinetic curves significantly, but their ratio is an important parameter. The simulated curves shown in Figure 1c and Figure 1d were obtained with the $k_{Ac}/k_P$ values equal to 0.5 and 0.2 for 273 and 253 K respectively.

Comparing simulated kinetic curves to the experimental results one can conclude that they are in good qualitative agreement. The simulated kinetics demonstrates sharper start of the reaction that is due to the applied assumption of the instant achievement of the equilibrium between various oligomers of the product. The simulation of the kinetic curves also confirms the validity of the applied estimation of the order of magnitude of the aldehyde decay rate constants.

Thus, we conclude that the experimentally detected acetal species forms in the off-loop of the catalytic cycle and is not an important intermediate in the process of the ee amplification. On the other hand, this observation is in agreement with the catalytic cycle outlined in our previous work,[25] since it implies the formation of the monomeric product that is essential for the possibility to trap the acetal in the form of $P_3$·Ac (Scheme 8).

## Computational Details

Computations were carried out using the hybrid B3LYP Becke functional[39–41] with 6-31G* basis set as implemented in the Gaussian 09 software package.[42] The solvent influence has been accounted for by carrying out optimizations in the CPCM force field (toluene).

## Supporting Information

Describe concisely what is in the material. This material is available electronically on J-STAGE.

## References


1 K. Soai, T. Shibata, H. Morioka, K. Choji, *Nature* **1995**, *378*, 767.
2 K. Soai, T. Shibata, I. Sato, *Acc. Chem. Res.* **2000**, *33*, 382.
3 K. Soai, T. Kawasaki, *Chirality* **2006**, *18*, 469.
4 K. Soai, T. Kawasaki, *Top. Curr. Chem.* **2008**, *284*, 1.
5 T. Kawasaki, K. Soai, *Bull. Chem. Soc. Jpn.* **2011**, *84*, 879.
6 K. Soai, T. Shibata, Y. Kowata, JP-Kokai 9-268179, **1997**.
7 V. I. Goldanskii, V. V. Kuzmin, *Z. Phys. Chem. (Leipz.)* **1988**, *269*, 216.

8 K. Mislow, *Collect. Czech. Chem. Commun.* **2003**, *68*, 849.
9 L. Caglioti, C. Hajdu, O. Holczknecht, L. Zékány, C. Zucchi, K. Micskei, G. Pályi, *Viva Orig.* **2006**, *34*, 62.
10 Y. Saito, H. Hyuga, *Rev. Mod. Phys.* **2013**, *85*, 603.
11 F. C. Frank, *Biochim. Biophys. Acta* **1953**, *11*, 459.
12 V. Avetisov, V. Goldanskii, *Proc. Natl. Acad. Sci. U.S.A.* **1996**, *93*, 11435.
13 D. G. Blackmond, C. R. McMillan, S. Ramdeehul, A. Schorm, J. M. Brown, *J. Am. Chem. Soc.* **2001**, *123*, 10103.
14 F. G. Buono, D. G. Blackmond, *J. Am. Chem. Soc.* **2003**, *125*, 8978.
15 T. Buhse, *Tetrahedron: Asymmetry* **2003**, *14*, 1055.
16 J. R. Islas, D. Lavabre, J.-M. Grevy, R. H. Lamoneda, H. R. Cabrera, J.-C. Micheau, T. Buhse, *Proc. Natl. Acad. Sci. U.S.A.* **2005**, *102*, 13743.
17 D. G. Blackmond, *Tetrahedron: Asymmetry* **2006**, *17*, 584.
18 J. R. Islas, T. Buhse, *J. Mex. Chem. Soc.* **2007**, *51*, 117.
19 J. M. Ribó, D. Hochberg, *Phys. Lett. A* **2008**, *373*, 111.
20 J. Crusats, D. Hochberg, A. Moyano, J. M. Ribó, *ChemPhysChem* **2009**, *10*, 2123.
21 J.-C. Micheau, J.-M. Cruz, C. Coudret, T. Buhse, *ChemPhysChem* **2010**, *11*, 3417.
22 D. G. Blackmond, *Tetrahedron: Asymmetry* **2010**, *21*, 1630.
23 E. Dóka, G. Lente, *J. Am. Chem. Soc.* **2011**, *133*, 17878.
24 T. Gehring, M. Quaranta, B. Odell, D. G. Blackmond, J. M. Brown, *Angew. Chem., Int. Ed.* **2012**, *51*, 9539.
25 I. D. Gridnev, A. Kh. Vorobiev, *ACS Catal.* **2012**, *2*, 2137.
26 A. Armstrong, R. A. Boto, P. Dingwall, J. Contreras-García, M. J. Harvey, N. J. Mason, H. S. Rzepa, *Chem. Sci.* **2014**, *5*, 2057.
27 U. Gellrich, D. Himmel, M. Meuwly, B. Breit, *Chem.—Eur. J.* **2013**, *19*, 16272.
28 W. M. C. Sameera, F. Maseras, *Wiley Interdiscip. Rev.: Comput. Mol. Sci.* **2012**, *2*, 375.
29 P. A. Dub, O. A. Filippov, N. V. Belkova, M. Rodrigez-Zubiri, R. Poli, *J. Phys. Chem. A* **2009**, *113*, 6348.
30 A. Hamza, G. Schubert, T. Soós, I. Pápai, *J. Am. Chem. Soc.* **2006**, *128*, 13151.
31 P. A. Dub, N. J. Henson, R. L. Martin, J. C. Gordon, *J. Am. Chem. Soc.* **2014**, *136*, 3505.
32 I. D. Gridnev, M. Watanabe, H. Wang, T. Ikariya, *J. Am. Chem. Soc.* **2010**, *132*, 16637.
33 I. D. Gridnev, Y. Liu, T. Imamoto, *ACS Catal.* **2014**, *4*, 203.
34 Y. Liu, I. D. Gridnev, W. Zhang, *Angew. Chem., Int. Ed.* **2014**, *53*, 1901.
35 I. D. Gridnev, J. M. Serafimov, J. M. Brown, *Angew. Chem., Int. Ed.* **2004**, *43*, 4884.
36 I. D. Gridnev, *Chem. Lett.* **2006**, *35*, 148.
37 J. Klankermayer, I. D. Gridnev, J. M. Brown, *Chem. Commun.* **2007**, 3151.
38 J. M. Brown, I. D. Gridnev, J. Klankermayer, *Top. Curr. Chem.* **2008**, *284*, 35.
39 A. D. Becke, *J. Chem. Phys.* **1993**, *98*, 1372.
40 A. D. Becke, *J. Chem. Phys.* **1993**, *98*, 5648.
41 C. Lee, W. Yang, R. G. Parr, *Phys. Rev. B* **1988**, *37*, 785.
42 M. J. Frisch, *et al.*, *Gaussian 09 (Revision C.01)*, Gaussian, Inc., Wallingford CT, **2010**.